Neuroscience Letters 682 (2018) 50–55

Contents lists available at ScienceDirect

Neuroscience Letters

journal homepage: www.elsevier.com/locate/neulet

Research article

Chemical chaperone 4-phenylbutylate reduces mutant protein accumulation in the endoplasmic reticulum of arginine vasopressin neurons in a mouse model for familial neurohypophysial diabetes insipidus

Masayoshi Tochiya[a], Daisuke Hagiwara[a,*,1], Yoshinori Azuma[a], Takashi Miyata[a], Yoshiaki Morishita[a], Hidetaka Suga[a], Takeshi Onoue[a], Taku Tsunekawa[a], Hiroshi Takagi[a], Yoshihiro Ito[a], Shintaro Iwama[a,b], Motomitsu Goto[a], Ryoichi Banno[a], Hiroshi Arima[a,*]

[a] Department of Endocrinology and Diabetes, Nagoya University Graduate School of Medicine, 65 Tsurumai-cho, Showa-ku, Nagoya, 466-8550, Japan
[b] Research Center of Health, Physical Fitness and Sports, Nagoya University, Nagoya, 464-8601, Japan

ARTICLE INFO

Keywords:
Familial neurohypophysial diabetes insipidus (FNDI)
4-Phenylbutylate (4-PBA)
Endoplasmic reticulum (ER) stress
Endoplasmic reticulum-associated compartment (ERAC)
Arginine vasopressin (AVP)

ABSTRACT

Familial neurohypophysial diabetes insipidus (FNDI), characterized by progressive polyuria and loss of arginine vasopressin (AVP) neurons, is an autosomal dominant disorder caused by *AVP* gene mutations. Our previous studies with FNDI model mice demonstrated that mutant proteins accumulated in the endoplasmic reticulum (ER) of AVP neurons. Here, we examined therapeutic effects of the chemical chaperone 4-phenylbutylate (4-PBA) in FNDI mice. Treatment with 4-PBA reduced mutant protein accumulation in the ER of FNDI mice and increased AVP release, leading to reduced urine volumes. Furthermore, AVP neuron loss under salt loading was attenuated by 4-PBA treatment. These data suggest that 4-PBA ameliorated mutant protein accumulation in the ER of AVP neurons and thereby prevented FNDI phenotype progression.

1. Introduction

Arginine vasopressin (AVP), an antidiuretic hormone, is synthesized in magnocellular neurons of the supraoptic (SON) and paraventricular nuclei (PVN) in the hypothalamus [4]. The *AVP* gene encodes a signal peptide, AVP, the AVP carrier protein neurophysin II (NPII), and a glycoprotein, also referred to as copeptin [34]. Prepro-AVP is truncated to pro-AVP upon removal of the signal peptide, and pro-AVP is folded into its native conformation in the endoplasmic reticulum (ER) [5]. After posttranslational processing in the ER, the pro-AVP is packed into secretory granules in the Golgi apparatus. AVP, NPII, and glycoprotein are cleaved from pro-AVP in the vesicle during transport to the posterior pituitary, from which AVP is released into the systemic circulation in response to changes in plasma osmolality and blood pressure [5,6].

Familial neurohypophysial diabetes insipidus (FNDI) is an autosomal dominant disorder caused by mutations in the *AVP* gene locus, mostly in the NPII-coding region [1]. FNDI is characterized by progressive polyuria due to AVP deficiency. We previously generated FNDI model mice that recapitulated the FNDI phenotype seen in humans [14]. Analyses of the FNDI mice revealed that ER stress due to accumulation of mutant AVP precursors in the ER is the main pathogenesis of FNDI [14,27]. Morphological examinations demonstrated that protein aggregates were confined to a certain compartment of the ER, ER-associated compartment (ERAC), in AVP neurons of the SON [13]. Furthermore, protein aggregates were scattered throughout the dilated ER lumen when FNDI mice were dehydrated, which worsened the FNDI phenotype and finally caused autophagy-associated cell death of AVP neurons [13].

The ER is an organelle that is mainly responsible for synthesis, folding, assembly, and transport of proteins [16]. Accumulation of misfolded and unfolded proteins leads to ER stress [35], which causes unfolded protein response including upregulation of ER chaperones [32] such as immunoglobulin heavy chain binding protein (BiP) [20] in order to cope with ER stress, while prolonged ER stress could finally lead to cell death [37]. ER stress has been implicated in a wide

Abbreviations: FNDI, familial neurohypophysial diabetes insipidus; AVP, arginine vasopressin; ER, endoplasmic reticulum; 4-PBA, 4-phenylbutylate; SON, supraoptic nucleus; PVN, paraventricular nucleus; NPII, neurophysin II; ERAC, endoplasmic reticulum-associated compartment; BiP, immunoglobulin heavy chain binding protein; PFA, paraformaldehyde; SCN, suprachiasmatic nucleus; NIH, National Institutes of Health; AU, arbitrary units

* Corresponding authors.
E-mail addresses: d-hagiwara@med.nagoya-u.ac.jp (D. Hagiwara), arima105@med.nagoya-u.ac.jp (H. Arima).
[1] Present address: Schaller Research Group on Neuropeptides, German Cancer Research Center (DKFZ), Heidelberg, 69120, Germany.

https://doi.org/10.1016/j.neulet.2018.06.013
Received 13 February 2018; Received in revised form 28 May 2018; Accepted 6 June 2018
Available online 07 June 2018
0304-3940/

spectrum of disorders, including neurodegenerative diseases [24], cerebral ischemia [38], depression [15], diabetes mellitus [28], and cancer [39]. Several studies have shown that ER stress is reduced in animal models treated with chemical chaperones such as 4-phenylbutylate (4-PBA) [3,25,29,31]. Furthermore, 4-PBA was shown to reduce protein accumulation in the ER in various *in vitro* models [9,21,33,36].

In the present study, we examined the effects of 4-PBA on progressive polyuria and loss of AVP neurons, as well as accumulation of mutant proteins in the ER together with BiP expression, as a marker of ER stress [22], in AVP neurons of FNDI mice.

2. Materials and methods

2.1. Animals

FNDI mice heterozygous for the mutant *Avp* gene (Cys98stop) were generated previously [14]. All FNDI mice in the present study were backcrossed over 15 generations into the C57BL/6 J background. C57BL/6 J mice were purchased from Chubu Science Materials (Nagoya, Japan). Mice were maintained under controlled conditions (23.0 ± 0.5 °C, lights on 09:00 to 21:00), and male mice were used in the experiments. All procedures were approved by the Animal Experimentation Committee of the Nagoya University Graduate School of Medicine and performed in accordance with institutional guidelines for animal care and use.

2.2. 4-PBA administration

Two-month-old mice were divided into control and 4-PBA groups. Mice in the 4-PBA group were treated with oral administration of 4-PBA (1 g/kg/day, Wako Pure Chemical Industries, Osaka, Japan) for 28 days. In experiments involving 4-PBA administration under salt loading conditions, 3-month-old mice were given 2% saline orally *ad libitum* with or without oral administration of 4-PBA (1 g/kg/day) for 7 days. The dosage of 4-PBA employed in this study was determined based on previous studies [17,29].

2.3. Measurements of urine volume and AVP

Mice were housed in metabolic cages, and 24-hour pooled urine was collected and assessed throughout the experimental period. Urine AVP levels were measured with a radioimmunoassay kit (AVP kit YAMASA; Yamasa Corporation, Chiba, Japan).

2.4. Brain collection for immunohistochemistry and in situ hybridization

Mice were deeply anesthetized and transcardially perfused with a cold fixative containing 4% paraformaldehyde (PFA) in PBS, pH 7.4. After fixation, brains were removed and immersed in the same fixative for 3 h at 4 °C. Brains were kept in PBS containing 10–20% sucrose at 4 °C for cryoprotection. They were then embedded in Tissue-Tek O.C.T. compound (Sakura Finetechnical, Tokyo, Japan) and stored at −80 °C until sectioning. Brains were cut into 16-μm sections on a cryostat at −20 °C, thaw-mounted on Superfrost Plus microscope slides (Matsunami Glass Ind., Osaka, Japan), and stored at −80 °C until either immunohistochemical analysis or *in situ* hybridization.

2.5. Immunohistochemistry

The frozen sections were washed with PBS for 15 min and then incubated with rabbit anti-mutant NPII antibody (1:1000) [14], in PBS with 0.3% Triton X-100 and 1% normal goat serum overnight at 4 °C. After rinsing with PBS, the primary antibody was probed using biotinylated goat anti-rabbit IgG (H + L) (1:200, BA-1000; Vector Laboratories, Burlingame, CA, USA) for 3 h at room temperature. The sections were washed in PBS and then incubated with avidin-biotin complex solution (1:100, Vectastatin ABC kit, PK-4000; Vector Laboratories) for 90 min at room temperature before immersion in PBS containing 0.1% 3,3′-diaminobenzidine dihydrochloride (Sigma-Aldrich, St. Louis, MO, USA). Antibody-binding sites were visualized upon addition of 0.004% hydrogen peroxide. NPII-expressing cells were counted and the number and diameter of inclusion bodies were measured using an Olympus DP73 digital camera system and an Olympus BX51 microscope equipped with cellSens Software (Olympus, Tokyo, Japan). The best-matched slices at 0.70 mm (SON), 0.82 mm (PVN), and 0.58 mm [suprachiasmatic nucleus (SCN)] caudal from the bregma, according to the brain atlas [30], were chosen from each mouse for analysis. The numbers of AVP neurons and inclusion bodies in each nucleus were counted, and the mean values in each mouse were subjected to statistical analyses.

2.6. Electron microscopy

Mice were deeply anesthetized and transcardially perfused with 4% PFA in PBS. Brains were dissected and cut into 100-μm sections on a vibratome (VT1200 S; Leica Biosystems, Wetzlar, Germany). The sections were fixed in a mixture of 2% PFA and 2.5% glutaraldehyde in PBS overnight at 4 °C, followed by postfixation with 2% osmium tetroxide for 20 min at 4 °C. Each section was dehydrated in a graded ethanol series, treated with propylene oxide, and embedded in epoxy resin (TAAB 812 resin; TAAB Laboratories Equipment, Aldermaston, UK). The resin was polymerized for 48 h at 60 °C. Ultrathin sections (70-nm thickness) including the SON were prepared using an ultramicrotome with a diamond knife (Reichert Ultracut S; Leica Biosystems) and counterstained with uranyl acetate and lead citrate before analysis with an electron microscope (JEM-1400EX; JEOL, Tokyo, Japan).

2.7. In situ hybridization and quantification

The *Avp* exonic probe was kindly provided by Dr. Harold Gainer [National Institutes of Health (NIH)] and the exonic probe of immunoglobulin heavy chain binding protein (BiP) was created from a 922-bp fragment containing bases 852 to 1773 of the mouse *Bip* cDNA as reported previously [12]. Radiolabeled antisense probes for *Avp* and *Bip* mRNA were synthesized using 55 μCi [^{35}S]UTP and 171 μCi [^{35}S]CTP (PerkinElmer Life Sciences, Waltham, MA, USA), the Riboprobe Combination System (Promega, Madison, WI, USA), 15 U of RNasin, 1 μg linearized template, and 15 U SP6 RNA polymerase. After incubation at 42 °C for 60 min, the cDNA templates were digested with DNase for 10 min at 37 °C. Radiolabeled RNA products were purified using Quick Spin Columns for radiolabeled RNA purification (Roche Diagnostics, Basel, Switzerland), precipitated with ethanol, and resuspended in 100 μl 10 mM Tris-HCl, pH 7.5 containing 20 mM dithiothreitol. Prehybridization, hybridization, and posthybridization procedures were performed as described previously [2]. The sections were exposed to BioMax MR film (Carestream Health, Rochester, NY, USA) for 4 h (*Avp* mRNA) or 48 h (*Bip* mRNA). The expression levels of *Avp* and *Bip* mRNA in the SON and PVN were quantified measuring of the integrated optimal densities (optical densities × area) of the film images using ImageJ software (NIH) and expressed in arbitrary units (AU).

2.8. Statistical analysis

The statistical significance of differences among groups was analyzed by an unpaired *t* test, log-rank test, one-way ANOVA, or two-way ANOVA, with repeated measures followed by the Bonferroni test as appropriate. Results are expressed as means ± SE, and differences were considered statistically significant at $P < 0.05$.

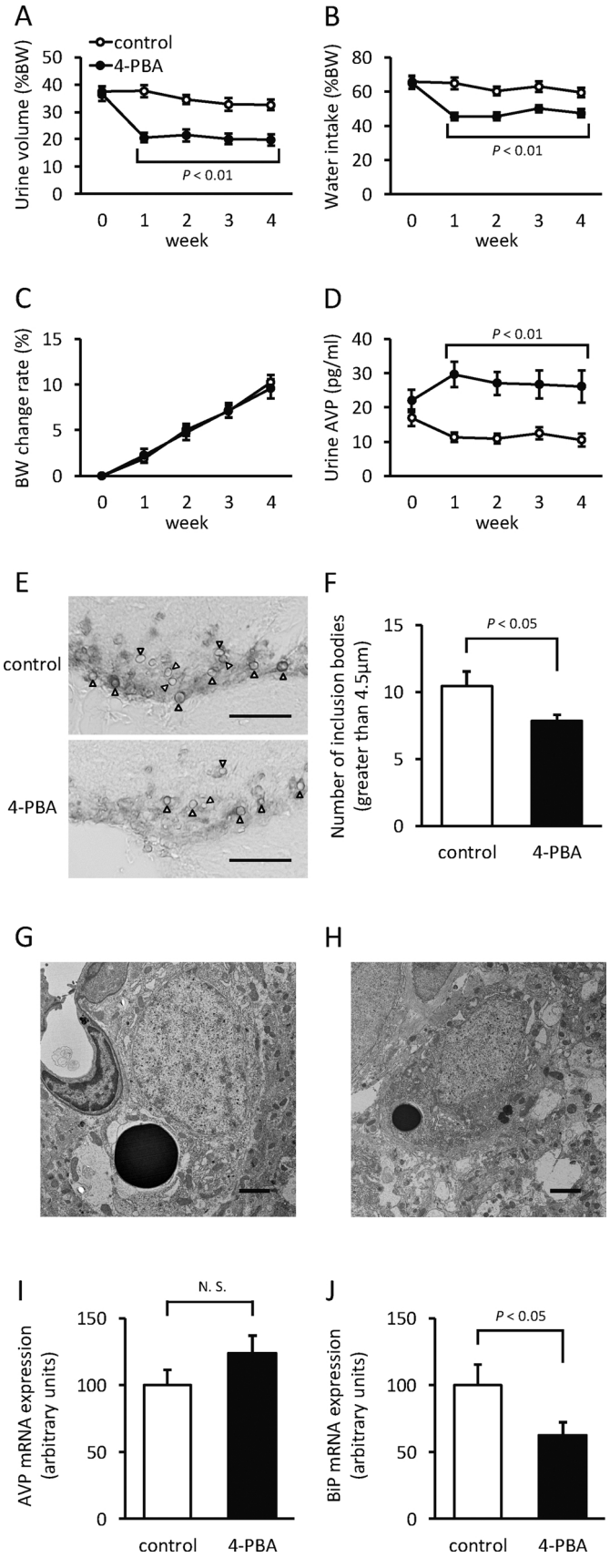

Fig. 1. Effects of 4-PBA on phenotype, inclusion bodies, and *Avp* and *Bip* mRNA expression in the SON of FNDI mice. Urine volumes (A), water intake (B), rate of body weight (BW) change (C), and urine AVP (D) of FNDI mice in control (open circles) and 4-PBA groups (closed circles). Representative photographs of immunohistochemical staining for mutant NPII of the SON (E) and the number of inclusion bodies with a diameter > 4.5 μm in the SON (F) of 3-month-old FNDI mice in the control and 4-PBA groups. Representative electron microscopic images of AVP neurons in the SON of 3-month-old FNDI mice in the control (G) and 4-PBA groups (H). mRNA expression levels of *Avp* (I) and *Bip* (J) in the SON of 3-month-old FNDI mice in the control and 4-PBA groups. Results are expressed as means ± SE ($n = 12$). Arrowheads, inclusion bodies. Scale bars, 50 μm (E) and 2 μm (G, H). N.S., not significant.

3. Results

3.1. The chemical chaperone 4-PBA decreased urine volume in FNDI mice

In FNDI mice, urine volumes and water intake significantly decreased in the 4-PBA group compared to the control group throughout the treatment (Fig. 1A and B). There were no significant differences in body weight between the control and 4-PBA groups (Fig. 1C). However, urine AVP levels significantly increased in the 4-PBA group relative to the control group (Fig. 1D). On the other hand, there were no significant differences in urine volumes, water intake, or urine AVP between control and 4-PBA groups in wild-type mice (Fig. S1).

3.2. 4-PBA reduced inclusion bodies and Bip mRNA levels in AVP neurons of FNDI mice

The number of inclusion bodies having diameters > 4.5 μm (the mean size in the 3-month-old FNDI mice [13]) was decreased in the 4-PBA group compared to the control group (SON, Fig. 1E and F; PVN, control 8.33 ± 0.51, 4-PBA 6.67 ± 0.33, $P = 0.011$). These data suggest that aggregates were reduced in size following 4-PBA treatment. Representative photographs of electron microscopic analyses are shown in Fig. 1G and H. However, at 3 months of age the control and 4-PBA FNDI mice showed no significant differences in *Avp* mRNA expression levels (SON, Fig. 1I; PVN, control 100.00 ± 24.36 AU, 4-PBA 101.55 ± 23.73 AU, $P = 0.96$), whereas the expression levels of *Bip* mRNA significantly decreased in the 4-PBA group relative to the control group (SON, Fig. 1J; PVN, control 100.00 ± 18.96 AU, 4-PBA 57.48 ± 8.99 AU, $P = 0.023$).

3.3. 4-PBA attenuated increases in urine volume under salt loading in FNDI mice

Whereas urine volumes and water intake increased and body weight decreased in 3-month-old FNDI mice given 2% saline in both control and 4-PBA groups, these changes were significantly attenuated by 4-PBA treatment (Fig. 2A–C). Urine AVP levels markedly increased on day 1 and then subsequently decreased in both groups, however the AVP levels were significantly higher in the 4-PBA group compared to the control group on days 2 and 3 (Fig. 2D).

3.4. 4-PBA maintained ERAC and attenuated Bip mRNA expression in AVP neurons under salt loading in FNDI mice

The numbers of AVP neurons in both control and 4-PBA FNDI mice were similar under salt-loading conditions for 3 days (SON, Fig. 2E; PVN, day 0 70.17 ± 3.87, control day 3 75.57 ± 5.43, 4-PBA day 3 81.57 ± 4.81, $P = 0.29$). However, there were fewer inclusion bodies in the control group relative to the 4-PBA in FNDI mice salt-loaded for 3 days (SON, Fig. 2F; PVN, day 0 8.33 ± 0.51, control day 3 5.00 ± 0.53, 4-PBA day 3 6.14 ± 0.26, $P = 0.034$). Electron microscopic examination revealed that protein aggregates were completely scattered throughout the dilated ER lumen in some AVP neurons of

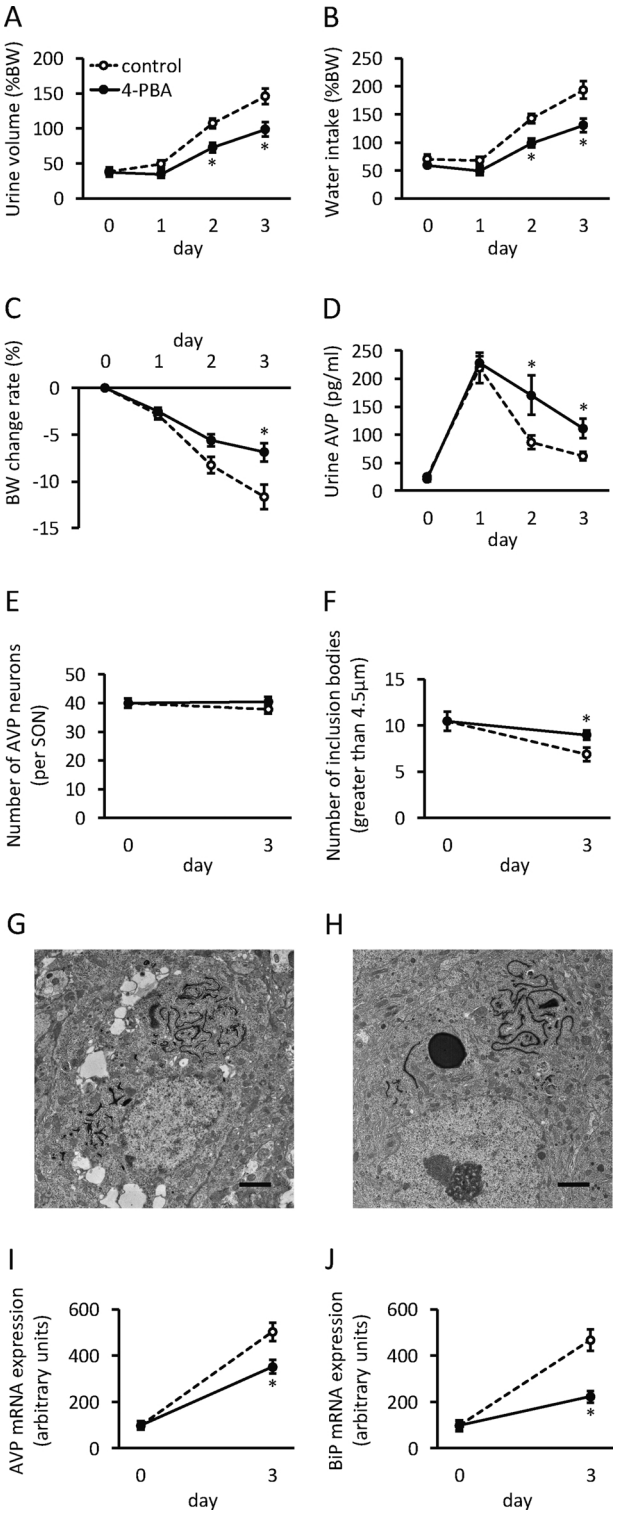

Fig. 2. Effects of 4-PBA on phenotype, number of AVP neurons, inclusion bodies, and *Avp* and *Bip* mRNA expression in the SON of FNDI mice under salt loading. Urine volumes (A), water intake (B), rate of BW change (C), urine AVP (D), and number of AVP neurons (E) and inclusion bodies (F) in the SON of 3-month-old FNDI mice subjected to 2% saline (control) and 2% saline with 4-PBA (4-PBA). Representative electron microscopic images of AVP neurons in the SON of FNDI mice treated with salt loading for 3 days in the control (G) and 4-PBA (H) groups. mRNA expression levels of *Avp* (I) and *Bip* (*J*) in the SON of FNDI mice in the control and 4-PBA groups. Control group, open circles and dashed line; 4-PBA group, closed circles and solid line. Results are expressed as means ± SE ($n = 6–12$). Scale bars, 2 μm. *$P < 0.05$ compared with the control group.

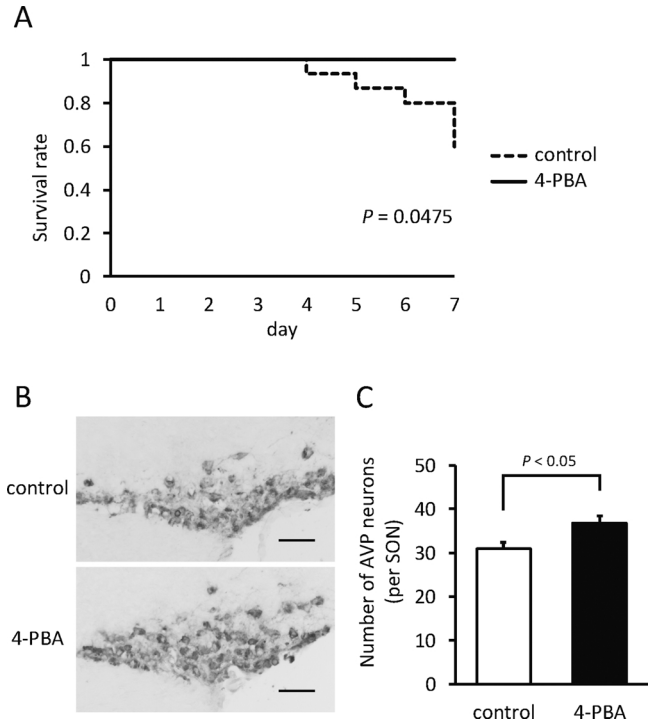

Fig. 3. Effects of 4-PBA on the survival rate and number of AVP neurons in the SON of FNDI mice under salt loading. (A) Kaplan-Meier survival curves for 3-month-old FNDI mice subjected to 2% saline (control, $n = 15$) and 2% saline with 4-PBA (4-PBA, $n = 8$). Representative photographs of immunohistochemical staining for mutant NPII of the SON (B) and the number of AVP neurons in the SON (C) of FNDI mice salt-loaded for 7 days in the control and 4-PBA groups. Results are expressed as means ± SE ($n = 7–9$). Scale bars, 50 μm.

FNDI mice salt-loaded for 3 days in the control group (Fig. 2G), whereas AVP neurons with partially maintained ERAC were observed in the 4-PBA group (Fig. 2H). The *Avp* and *Bip* mRNA expression levels in FNDI mice salt-loaded for 3 days significantly increased in the control group, whereas this increase was significantly attenuated in the 4-PBA group (SON, Fig. 2I and *J*; PVN, *Avp* mRNA, day 0 100.00 ± 24.36 AU, control day 3 1005.21 ± 149.32 AU, 4-PBA day 3 700.39 ± 58.94 AU, $P = 0.033$, *Bip* mRNA, day 0 100.00 ± 18.96 AU, control day 3 302.87 ± 19.62 AU, 4-PBA day 3 220.56 ± 20.40 AU, $P = 0.0056$).

3.5. 4-PBA prevented AVP neuron loss under salt loading in FNDI mice

Under 2% saline administration, 6/15 (40%) FNDI mice in the control group died 4–7 days after beginning the treatment, whereas all FNDI mice in the 4-PBA group survived throughout the treatment period (Fig. 3A). The death was probably caused by severe dehydration, as suggested by more body weight loss in the control compared to the 4-PBA group (Fig. 2C). On day 7, the number of AVP neurons in the surviving control group mice was significantly lower than that of the 4-PBA group (SON, Fig. 3B and C; PVN, control 64.25 ± 3.17, 4-PBA 75.50 ± 5.02, $P = 0.044$). On the other hand, there were no significant differences in the number of AVP neurons in the SCN (day 0 135.75 ± 6.84, control day 7 139.70 ± 8.65, 4-PBA day 7 133.00 ± 6.76, $P = 0.83$).

4. Discussion

In the present study, we showed that the chemical chaperone 4-PBA increased AVP secretion, reduced urine volumes, and prevented AVP neuronal loss in FNDI mice. Our data also demonstrated that mutant

protein accumulation in the ER of AVP neurons was reduced by 4-PBA treatment *in vivo*.

Although ER stress has been implicated in the pathogenesis of many diseases [18,41], only limited numbers of animal models exist that show accumulation of misfolded proteins in the ER. The diseases for these models include α_1-antitrypsin deficiency [7], familial encephalopathy with neuroserpin inclusion body [11], and seipinopathy [40]. Several studies have examined the effects of chemical chaperones in animal models displaying ER stress [8,19]. 4-PBA has been used in animal models of neurodegenerative diseases [10,42] as this compound reportedly permeates the blood brain barrier [23,26]. However, no studies have shown that chemical chaperones such as 4-PBA can reduce the amount of misfolded protein accumulation in the ER *in vivo*.

Our previous studies demonstrated that intracellular inclusion bodies formed in the AVP neurons of FNDI mice, and that the size and number increased in parallel with urine volumes until the mice were at least 6 months old [14]. Electron microscopic observations revealed that massive protein aggregates were confined to a certain ER compartment (i.e. ERAC) in AVP neurons [13]. In the current study, 4-PBA reduced the number of inclusion bodies with a diameter > 4.5 μm, suggesting that accumulation of mutant proteins in the ER was reduced by 4-PBA treatment. Furthermore, AVP secretion was increased and urine volumes were decreased by the treatment. Thus, to our knowledge, this is the first demonstration that 4-PBA treatment could decrease accumulation of misfolded proteins in the ER of neurons, and this decrease is accompanied by ameliorated polyuria, a representative phenotype of FNDI.

We previously showed that age and intermittent water deprivation were associated with impeded confinement of mutant proteins in the ERAC, characterized by aggregates scattered throughout the ER lumen, and subsequent loss of AVP neurons through autophagy-associated cell death [13]. In the present study, we gave 2% saline to FNDI mice orally to accelerate development of the FNDI phenotype, and found that ERAC formation was impeded within 3 days of initiating the treatment. With this protocol, we showed that 4-PBA could maintain ERAC formation and AVP secretion. Furthermore, the number of AVP neurons was significantly higher in the 4-PBA group compared to the control group on day 7, suggesting that 4-PBA prevented cell death of AVP neurons under dehydration.

Our previous study showed that *Avp* and *Bip* mRNA are colocalized in the SON, and that both mRNAs increase under dehydration [12]. As BiP expression has been used as a marker of ER stress [22], we examined the effect of 4-PBA on *Bip* mRNA in the current study and demonstrated that its expression was significantly reduced with 4-PBA treatment. Our data also showed that 4-PBA increased AVP secretion in FNDI mice, suggesting that it enhanced the efficiency of posttranslational AVP processing by reducing mutant protein accumulation. Such improvement in ER stress could decrease the load for AVP neurons and could explain why *Avp* mRNA expression was decreased by 4-PBA treatment.

In conclusion, our data demonstrated that 4-PBA treatment in FNDI mice reduced mutant protein accumulation in the ER and increased AVP secretion, leading to ameliorated polyuria. Our data also showed that 4-PBA could reduce accumulation of misfolded proteins in the ER of neurons *in vivo*, suggesting that chemical chaperones that permeate the blood brain barrier could be a therapeutic application for neurodegenerative diseases.

Acknowledgments

We thank Michiko Yamada and Koji Itakura for their helpful technical assistance. This work was supported by JSPS KAKENHI Grant Number JP15K19530 (to D. Hagiwara) and the Acceleration Program for Intractable Diseases Research utilizing Disease-specific iPS cells (to H. Suga) of the Research Center Network for Realization of Regenerative Medicine from Japan Agency for Medical Research and Development (AMED).

Appendix A. Supplementary data

Supplementary material related to this article can be found, in the online version, at doi:https://doi.org/10.1016/j.neulet.2018.06.013.

References

[1] H. Arima, Y. Azuma, Y. Morishita, D. Hagiwara, Central diabetes insipidus, Nagoya J. Med. Sci. 78 (2016) 349–358.
[2] Y. Azuma, D. Hagiwara, W. Lu, Y. Morishita, H. Suga, M. Goto, R. Banno, Y. Sugimura, S. Oyadomari, K. Mori, A. Shiota, N. Asai, M. Takahashi, Y. Oiso, H. Arima, Activating transcription factor 6α is required for the vasopressin neuron system to maintain water balance under dehydration in male mice, Endocrinology 155 (2014) 4905–4914.
[3] S. Basseri, S. Lhoták, A.M. Sharma, R.C. Austin, The chemical chaperone 4-phenylbutyrate inhibits adipogenesis by modulating the unfolded protein response, J. Lipid Res. 50 (2009) 2486–2501.
[4] G.W. Bisset, H.S. Chowdrey, Control of release of vasopressin by neuroendocrine reflexes, Q. J. Exp. Physiol. 73 (1988) 811–872.
[5] M.J. Brownstein, J.T. Russell, H. Gainer, Synthesis, transport, and release of posterior pituitary hormones, Science 207 (1980) 373–378.
[6] J.P. Burbach, S.M. Luckman, D. Murphy, H. Gainer, Gene regulation in the magnocellular hypothalamo-neurohypophysial system, Physiol. Rev. 81 (2001) 1197–1267.
[7] J.A. Burrows, L.K. Willis, D.H. Perlmutter, Chemical chaperones mediate increased secretion of mutant alpha 1-antitrypsin (alpha 1-AT) Z: A potential pharmacological strategy for prevention of liver injury and emphysema in alpha 1-AT deficiency, Proc. Natl. Acad. Sci. U. S. A. 97 (2000) 1796–1801.
[8] L. Cortez, V. Sim, The therapeutic potential of chemical chaperones in protein folding diseases, Prion 8 (2014).
[9] S.F. de Almeida, G. Picarote, J.V. Fleming, M. Carmo-Fonseca, J.E. Azevedo, M. de Sousa, Chemical chaperones reduce endoplasmic reticulum stress and prevent mutant HFE aggregate formation, J. Biol. Chem. 282 (2007) 27905–27912.
[10] G. Gardian, S.E. Browne, D.K. Choi, P. Klivenyi, J. Gregorio, J.K. Kubilus, H. Ryu, B. Langley, R.R. Ratan, R.J. Ferrante, M.F. Beal, Neuroprotective effects of phenylbutyrate in the N171-82Q transgenic mouse model of Huntington's disease, J. Biol. Chem. 280 (2005) 556–563.
[11] M.C. Hagen, J.R. Murrell, M.B. Delisle, E. Andermann, F. Andermann, M.C. Guiot, B. Ghetti, Encephalopathy with neuroserpin inclusion bodies presenting as progressive myoclonus epilepsy and associated with a novel mutation in the Proteinase Inhibitor 12 gene, Brain Pathol. 21 (2011) 575–582.
[12] D. Hagiwara, H. Arima, Y. Morishita, M. Goto, R. Banno, Y. Sugimura, Y. Oiso, BiP mRNA expression is upregulated by dehydration in vasopressin neurons in the hypothalamus in mice, Peptides 33 (2012) 346–350.
[13] D. Hagiwara, H. Arima, Y. Morishita, L. Wenjun, Y. Azuma, Y. Ito, H. Suga, M. Goto, R. Banno, Y. Sugimura, A. Shiota, N. Asai, M. Takahashi, Y. Oiso, Arginine vasopressin neuronal loss results from autophagy-associated cell death in a mouse model for familial neurohypophysial diabetes insipidus, Cell Death Dis. 5 (2014) e1148.
[14] M. Hayashi, H. Arima, N. Ozaki, Y. Morishita, M. Hiroi, H. Nagasaki, N. Kinoshita, M. Ueda, A. Shiota, Y. Oiso, Progressive polyuria without vasopressin neuron loss in a mouse model for familial neurohypophysial diabetes insipidus, Am. J. Physiol. Regul. Integr. Comp. Physiol. 296 (2009) R1641–1649.
[15] C. Kakiuchi, K. Iwamoto, M. Ishiwata, M. Bundo, T. Kasahara, I. Kusumi, T. Tsujita, Y. Okazaki, S. Nanko, H. Kunugi, T. Sasaki, T. Kato, Impaired feedback regulation of XBP1 as a genetic risk factor for bipolar disorder, Nat. Genet. 35 (2003) 171–175.
[16] R.J. Kaufman, Stress signaling from the lumen of the endoplasmic reticulum: coordination of gene transcriptional and translational controls, Genes Dev. 13 (1999) 1211–1233.
[17] E. Kemter, S. Sklenak, B. Rathkolb, M. Hrabě de Angelis, E. Wolf, B. Aigner, R. Wanke, No amelioration of uromodulin maturation and trafficking defect by sodium 4-phenylbutyrate in vivo: studies in mouse models of uromodulin-associated kidney disease, J. Biol. Chem. 289 (2014) 10715–10726.
[18] I. Kim, W. Xu, J.C. Reed, Cell death and endoplasmic reticulum stress: disease relevance and therapeutic opportunities, Nat. Rev. Drug Discov. 7 (2008) 1013–1030.
[19] P.S. Kolb, E.A. Ayaub, W. Zhou, V. Yum, J.G. Dickhout, K. Ask, The therapeutic effects of 4-phenylbutyric acid in maintaining proteostasis, Int. J. Biochem. Cell Biol. 61 (2015) 45–52.
[20] Y. Kozutsumi, M. Segal, K. Normington, M.J. Gething, J. Sambrook, The presence of malfolded proteins in the endoplasmic reticulum signals the induction of glucose-regulated proteins, Nature 332 (1988) 462–464.
[21] K. Kubota, Y. Niinuma, M. Kaneko, Y. Okuma, M. Sugai, T. Omura, M. Uesugi, T. Uehara, T. Hosoi, Y. Nomura, Suppressive effects of 4-phenylbutyrate on the aggregation of Pael receptors and endoplasmic reticulum stress, J. Neurochem. 97 (2006) 1259–1268.
[22] A.S. Lee, The ER chaperone and signaling regulator GRP78/BiP as a monitor of endoplasmic reticulum stress, Methods 35 (2005) 373–381.
[23] N.Y. Lee, Y.S. Kang, *In vivo* and *in vitro* evidence for brain uptake of 4-phenylbutyrate by the monocarboxylate transporter 1 (MCT1), Pharm. Res. 33 (2016) 1711–1722.
[24] D. Lindholm, H. Wootz, L. Korhonen, ER stress and neurodegenerative diseases, Cell Death Differ. 13 (2006) 385–392.

[25] S.H. Liu, C.C. Yang, D.C. Chan, C.T. Wu, L.P. Chen, J.W. Huang, K.Y. Hung, C.K. Chiang, Chemical chaperon 4-phenylbutyrate protects against the endoplasmic reticulum stress-mediated renal fibrosis in vivo and in vitro, Oncotarget 7 (2016) 22116–22127.
[26] Y.H. Loo, T. Fulton, H.M. Wisniewski, Vulnerability of the immature brain to phenylacetate intoxication: tissue permeability to phenylacetate, J. Neurochem. 32 (1979) 1697–1698.
[27] Y. Morishita, H. Arima, M. Hiroi, M. Hayashi, D. Hagiwara, N. Asai, N. Ozaki, Y. Sugimura, H. Nagasaki, A. Shiota, M. Takahashi, Y. Oiso, Poly(A) tail length of neurohypophysial hormones is shortened under endoplasmic reticulum stress, Endocrinology 152 (2011) 4846–4855.
[28] U. Ozcan, Q. Cao, E. Yilmaz, A.H. Lee, N.N. Iwakoshi, E. Ozdelen, G. Tuncman, C. Görgün, L.H. Glimcher, G.S. Hotamisligil, Endoplasmic reticulum stress links obesity, insulin action, and type 2 diabetes, Science 306 (2004) 457–461.
[29] U. Ozcan, E. Yilmaz, L. Ozcan, M. Furuhashi, E. Vaillancourt, R.O. Smith, C.Z. Görgün, G.S. Hotamisligil, Chemical chaperones reduce ER stress and restore glucose homeostasis in a mouse model of type 2 diabetes, Science 313 (2006) 1137–1140.
[30] G. Paxinos, K. Franklin, The Mouse Brain in Stereotaxic Coordinates, Academic Press, New York, 2000.
[31] X. Qi, T. Hosoi, Y. Okuma, M. Kaneko, Y. Nomura, Sodium 4-phenylbutyrate protects against cerebral ischemic injury, Mol. Pharmacol. 66 (2004) 899–908.
[32] D. Ron, P. Walter, Signal integration in the endoplasmic reticulum unfolded protein response, Nat. Rev. Mol. Cell Biol. 8 (2007) 519–529.
[33] R.C. Rubenstein, M.E. Egan, P.L. Zeitlin, In vitro pharmacologic restoration of CFTR-mediated chloride transport with sodium 4-phenylbutyrate in cystic fibrosis epithelial cells containing delta F508-CFTR, J. Clin. Invest. 100 (1997) 2457–2465.
[34] E. Sausville, D. Carney, J. Battey, The human vasopressin gene is linked to the oxytocin gene and is selectively expressed in a cultured lung cancer cell line, J. Biol. Chem. 260 (1985) 10236–10241.
[35] M. Schröder, R.J. Kaufman, ER stress and the unfolded protein response, Mutat. Res. 569 (2005) 29–63.
[36] Y. Song, G. Fang, H. Shen, H. Li, W. Yang, B. Pan, G. Huang, G. Lin, L. Ma, B. Willard, J. Gu, L. Zheng, Y. Wang, Human surfactant protein A2 gene mutations impair dimmer/trimer assembly leading to deficiency in protein sialylation and secretion, PLoS One 7 (2012) e46559.
[37] I. Tabas, D. Ron, Integrating the mechanisms of apoptosis induced by endoplasmic reticulum stress, Nat. Cell Biol. 13 (2011) 184–190.
[38] S. Tajiri, S. Oyadomari, S. Yano, M. Morioka, T. Gotoh, J.I. Hamada, Y. Ushio, M. Mori, Ischemia-induced neuronal cell death is mediated by the endoplasmic reticulum stress pathway involving CHOP, Cell Death Differ. 11 (2004) 403–415.
[39] T. Verfaillie, A.D. Garg, P. Agostinis, Targeting ER stress induced apoptosis and inflammation in cancer, Cancer Lett. 332 (2013) 249–264.
[40] T. Yagi, D. Ito, Y. Nihei, T. Ishihara, N. Suzuki, N88S seipin mutant transgenic mice develop features of seipinopathy/BSCL2-related motor neuron disease via endoplasmic reticulum stress, Hum. Mol. Genet. 20 (2011) 3831–3840.
[41] H. Yoshida, ER stress and diseases, FEBS J. 274 (2007) 630–658.
[42] W. Zhou, K. Bercury, J. Cummiskey, N. Luong, J. Lebin, C.R. Freed, Phenylbutyrate up-regulates the DJ-1 protein and protects neurons in cell culture and in animal models of Parkinson disease, J. Biol. Chem. 286 (2011) 14941–14951.

Figure S1

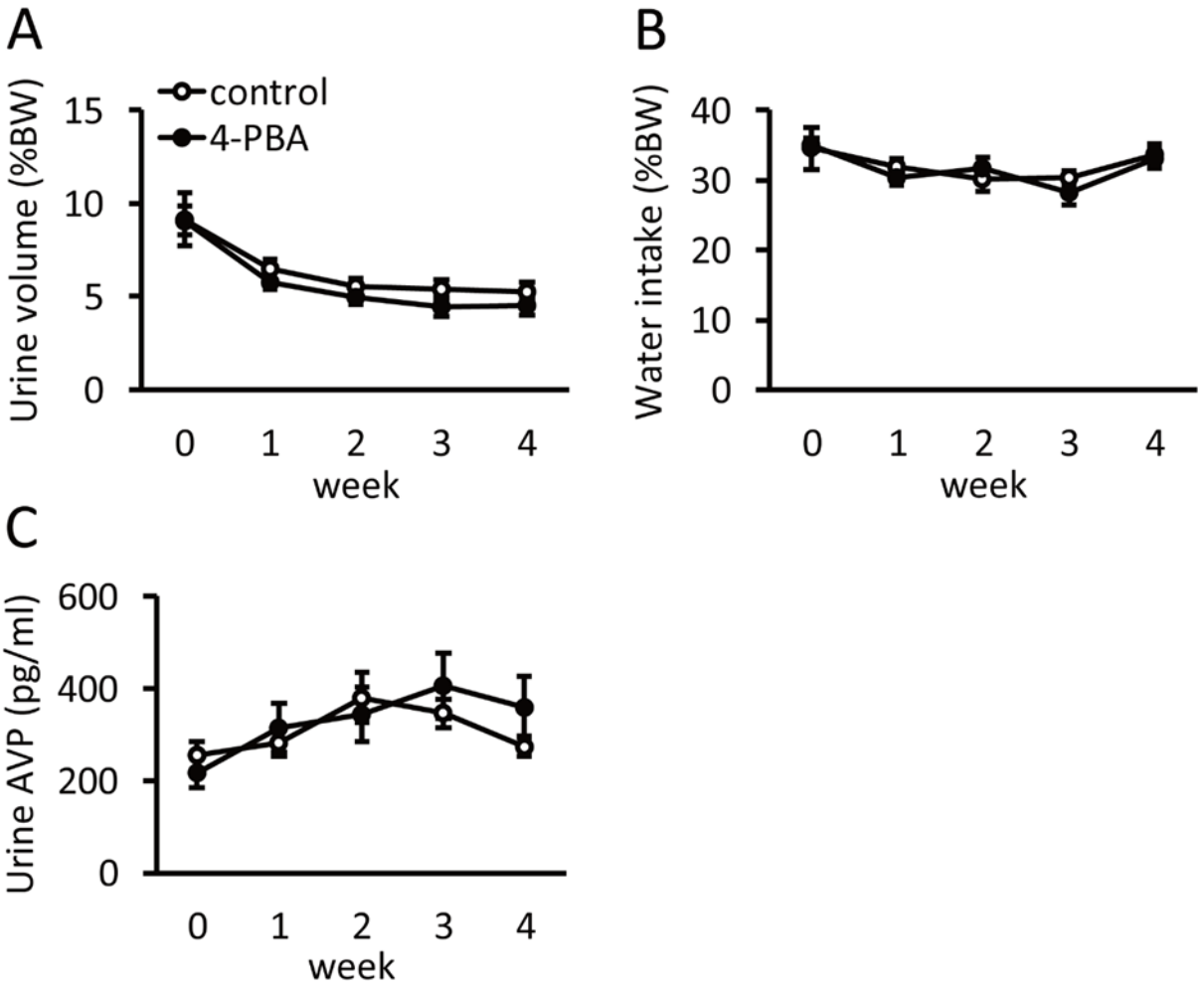

Fig. S1. Effects of 4-PBA on urine volumes (A), water intake (B), and urine AVP (C) of wild-type mice in control (open circles) and 4-PBA groups (closed circles). Results are expressed as means ± SE (*n* = 3-6).